# Nonlinear Analysis of Heated, Cambered Wings by the Matrix Force Method

WARNER LANSING*
*Grumman Aircraft Engineering Corporation, Bethpage, N. Y.*
IRVING W. JONES†
*Fairchild Stratos Corporation, Bayshore, N. Y.*
AND
PAUL RATNER‡
*Grumman Aircraft Engineering Corporation, Bethpage, N. Y.*

**The matrix-force method of redundant structure analysis is extended to handle the nonlinear behavior of heated, cambered wings. Effects specifically covered include 1) the change in flexibility which occurs when thermal stresses are present, 2) large deflections, and 3) initial camber and warp. The approach is a finite-element counterpart of Marguerre's formulation for the strain-displacement and equilibrium relations for shallow shells. An example is included to illustrate application of the method to wings and to indicate the nature and the magnitude of the effects being examined. Whereas the discussion is limited to cambered wings, the method is not restricted to structures of this type but actually applies equally well to shallow shells in general.**

## Nomenclature

$P_m$ = lateral applied load at $m$th panel point
$\epsilon_j$ = axial or shear strain at the $j$th member load in the unloaded, statically determinate structure
$q_i$ = member load; any load acting directly upon an individual member
$\delta_m$ = displacement at the $m$th panel point (from the cambered shape)
$\bar{\delta}_m$ = displacement of redundant structure at load $P_m$ due only to antisymmetric thermal strains and due only to bending about mean chord surface
$\Gamma_{im}$ = member-load influence coefficient in redundant structure; $i$th member load in the redundant structure due to a unit $m$th applied load
$A_{mn}$ = flexibility influence coefficient for linear deflection of the redundant structure; displacement at load $P_m$ due to a unit load $P_n$
$L_{ij}$ = geometric coefficient used in the unit analysis; displacement at $i$th member load due to a unit strain at the $j$th member load, both in the unloaded, statically determinate structure
$\Gamma_{ij}$ = member-load influence coefficient in redundant structure; $i$th member load in the redundant structure caused by a unit strain at the $j$th member load in the unloaded, statically determinate structure
$A_{mj}$ = flexibility influence coefficient for linear deflection of the redundant structure; displacement at the $m$th applied load in the redundant structure due to a unit strain at the $j$th member load in the unloaded, statically determinate structure
$\alpha$ = linear coefficient of thermal expansion
$T$ = change in temperature
$Z,Z'$ = lateral resultant forces in a spar segment and shear panel, respectively
$P'_m$ = the total lateral load sustained at the $m$th panel point due to membrane behavior alone
$\Delta_m$ = ordinate of the cambered surface at the $m$th panel point from a chosen reference plane
$K_{mn}$ = stiffness influence coefficient for linear deflection of the redundant structure or a component thereof
$\Delta K_{mn}$ = component of membrane stiffness, Eq. (19)

***Subscripts***

$i,j,k$ = member load
$r,s$ = redundant
$m,n,t$ = panel point, applied load, or displacement
$M$ = membrane component; symmetric about the mean chord surface
$B$ = bending component; antisymmetric about the mean chord surface

***Superscript***

$k$ = $k$th iteration

***Matrices***

$\{\ \}$ = column matrix
$\{\ \}$ = matrix with layers of columns
$[\ ]$ = rectangular matrix
 = matrix with layers of rectangular arrays
$[\ |$ = diagonal matrix
 = matrix with layers of diagonals

## Introduction

THE several finite-element structural-analysis methods currently in general use throughout the aerospace industry originally were developed with the linear analysis of airframes in mind; more recently they have been extended by a number of investigators to include various nonlinear structural effects. See, for example, Refs. 1–4.

The present effort treats the specific problem of a heated, cambered wing. The nonlinear feature in this case is the effect of finite deflections, rather than any material property consideration. Whereas the procedure was originated for low-aspect ratio wings and is discussed from this point of view herein, it is equally applicable to shallow shells in general,[5] the formulation of the strain-displacement and equilibrium relations being a finite element equivalent to that used by Marguerre.[6]

Presented at the IAS National Summer Meeting, Los Angeles, Calif., June 19–22, 1962; revision received April 26, 1963. This work was performed under the sponsorship of the Grumman Aircraft Engineering Corporation Advanced Development Program.

* Structural Methods Group Leader. Member AIAA.
† Structures Group Leader, Spacecraft Systems Division.
‡ Structural Methods Engineer.

Basically, the method consists of first carrying out two separate analyses, one for the bending behavior, the other for the membrane behavior. In so doing, the wing is idealized as consisting of a number of bars and shear panels. The output of the bending analysis is a conventional stiffness matrix that is independent of the lateral displacements. The membrane analysis, on the other hand, yields a stiffness matrix that is a function of the displacements. Its determination requires that one first assume a set of lateral displacements. From the two component stiffness matrices, one can assemble a matrix equation giving the total loading carried by the structure in the assumed deflected configuration. Thereafter, an iterative procedure is used to find the deflections that correspond to the actual applied loads. In the process, one of the outputs is a "tangent flexibility influence coefficient matrix," which gives the flexibility of the structure for small displacements about the deflected shape.

The less general case of an uncambered, heated airfoil or control surface has been described by the present authors in a previous paper.[7]

The plan of this paper is as follows: first, a very brief outline of the basic matrix-force method as it has previously been reported in the literature; next, a general discussion of the interaction between bending behavior and membrane behavior of a cambered wing; finally, some numerical results for a low aspect ratio, untapered box beam of constant depth, both with and without camber. From these results, it would appear that the root support condition can have an important bearing upon whether or not a cambered wing will exhibit pronounced nonlinear behavior.

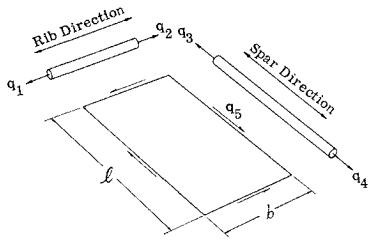


**Fig. 1 Shear panel and adjacent stringers**

Throughout the paper, the method is formulated for a structure with rectangular subdivisions. This is for convenience of presentation only; expressions of comparable accuracy can be obtained for parallelogram subdivisions as well.[7] A simplified engineering approximation of this same approach also can be used for the general case in which neither the spars nor the ribs are parallel.

## II. Review of Matrix-Force Method

### 1. Unit Load and Unit Strain Analysis

Throughout the matrix-force method, member-load distributions and deflections for a particular applied load condition are expressed in terms of their values for unit applied loads. These are the familiar influence coefficients. To extend the method to thermoelastic and other special type analyses, it is necessary to calculate two other influence coefficient matrices. The first expresses the load distributions in the redundant structure due to unit strains existing in the various members in the unloaded statically determinate state. The second, for deflections, is defined similarly. From these matrices, which will be designated $[\Gamma_{ij}]$ and $[A_{mj}]$, respectively, the member loads and deflections for a particular thermal gradient, for example, can be written as a superposition of the influence coefficients each multiplied by the appropriate thermal strain. Thermal strains in the statically determinate structure are calculated easily since the structure is stress free, and free thermal expansion is permitted.

There are four fundamental matrices required as input data for performing a unit load and unit strain analysis by the matrix-force method. These are

1) $[\gamma_{im}]$—the member loads in the statically determinate structure due to unit values of the applied loads;

2) $[\gamma_{ir}]$—the member loads in the statically determinate structure due to unit values of the redundants;

3) $[\alpha_{ij}]$—the flexibilities of the individual members making up the structure;

4) $[L_{ij}]$—strain-displacement factors for the individual members making up the structure.

These matrices can be assembled by hand or obtained from digital computer subroutines. (The subscripts $i,j$, and $k$ designating member loads can be considered interchangeable except within an equation, and the same is true for $m$, $n$, and $t$, panel point designations; e.g., $[\gamma_{im}] \equiv [\gamma_{jn}]$, etc.)

The member-load distribution due to unit applied loads, otherwise called the member-load influence coefficient matrix, and the flexibility influence coefficient matrix, can be calculated by a sequence of operations involving the just mentioned four matrices. The applicable formulas are expressed in various forms.[8–14] As for the unit strain influence coefficient matrices for load and deflection, the formulas, also given in some of the cited publications, are repeated in the notation of this paper as follows:

$$[\Gamma_{ik}] = -[\gamma_{ir}]([\gamma_{ir}]'[\alpha_{ij}][\gamma_{js}])^{-1}([\gamma_{js}]'[L_{jk}]) \equiv [\Gamma_{jk}] \equiv [\Gamma_{ij}]$$
$$[A_{mk}] = [\gamma_{im}]'([\alpha_{ij}][\Gamma_{jk}] + [L_{ik}]) \equiv [A_{mj}] \tag{1}$$

### 2. Member Load Distribution and Deflections

The formulas for the member-load distribution $\{q_i\}$ and deflections $\{\delta_m\}$ for a particular design condition consisting of applied loads $\{P_m\}$ and thermal strains $\{\epsilon_j\}$ readily can be written

$$\{q_i\} = [\Gamma_{im}]\{P_m\} + [\Gamma_{ij}]\{\epsilon_j\} \tag{2}$$

$$\{\delta_m\} = [A_{mn}]\{P_n\} + [A_{mj}]\{\epsilon_j\} \tag{3}$$

The component of deflection due only to temperature is termed $\{\bar{\delta}_m\}$ and will be useful as a separate quantity in a later part of the analysis.

$$\{\bar{\delta}_m\} = [A_{mj}]\{\epsilon_j\} \tag{4}$$

### 3. Lumped Stringer and Shear Panel Idealization

A multispar, multirib wing may be idealized as an assemblage of capstrips carrying axial load only, interconnected by shear panels that can carry tangential edge loads only. Using this approach, one lumps the covers into equivalent capstrips over the spars and ribs; the contributions of the spars and ribs themselves are calculated in the usual way and added in. If appropriate, intermediate shear lag members are introduced as well. Because of the shear panel assumption, the axial loads in the capstrips vary linearly from one panel point to the next.

Based upon this idealization, the member loads in the statically determinate structure may be obtained in any convenient way. The method suggested by Argyris and Kelsey,[10] and by Grzedzielski[11, 12] is recommended especially; it has worked out very well in a number of applications at Grumman.

The member flexibilities for a wing with parallel spars and parallel ribs normal to the spars can be obtained readily from Ref. 11. Refer to Fig. 1, which shows a single shear panel, together with two of its adjacent lumped stringers. For the case of uniform cross-sectional areas, the necessary expressions are as follows:

$$\alpha_{11} = 2\alpha_{12} = \alpha_{22} = b/3A_rE$$
$$\alpha_{33} = 2\alpha_{34} = \alpha_{44} = l/3A_sE$$
$$\alpha_{55} = bl/Gt$$
$$\alpha_{23} = -R_sR_r(\nu/Et)$$

In these formulas $A_s$ is the total lumped spar area in a section normal to the spar, whereas $R_s = (\frac{1}{2}bl)/A_s$. $A_r$ and $R_r$ are similarly defined. The stringer lengths are $b$ and $l$, $\nu$ is Poisson's ratio, and $E$ and $G$ are Young's modulus and the shear modulus of the material. The member flexibility $\alpha_{23}$ introduces Poisson's ratio coupling in the cover material.

Referring again to Fig. 1, the geometrical quantities required in the unit strain analysis are as follows:

$$L_{11} = 2L_{12} = L_{22} = b/3$$
$$L_{33} = 2L_{34} = L_{44} = l/3$$
$$L_{55} = bl$$

The strains, $\epsilon_1 \ldots \epsilon_5$, are the values associated with the corresponding member loads.

Formulas corresponding to those just mentioned but for a swept wing were given in a previous paper.[7] They were applied to a swept wing with uniform thickness and the results agreed favorably with published test results.

The bar and shear panel idealization also works very well for solid plates. See Ref. 7 for the case of a simply supported square plate subjected to lateral load.

## III. General Discussion of the Interaction

In the customary method for analyzing wings, one assumption implied is that the effects on flexibility of membrane stresses, such as those due to thermal gradients, can be neglected. This assumption, while usually being quite satisfactory, may lead to inaccurate predictions of flexibility as well as stresses if taken to be valid for a low aspect ratio wing that is fairly thin, especially if it has camber or warp.

In this section of the paper, general formulas are derived for the loading sustained by the structure due to bending and membrane action in an assumed deflected shape and under a given thermal environment. Also obtained are formulas for the corresponding stress distribution and the flexibility of the structure for small displacements about the deflected shape. The latter is stated by means of a matrix of "tangent flexibility influence coefficients" which is dependent upon the loading. In the following section an iterative procedure for finding the deflections that correspond to the actual applied loads is given.

The basis of the method is the treatment of stresses, deflections, and strains as a superposition of components symmetrical and antisymmetrical about the mean chord surface, the symmetrical components of the stresses and strains being identical in the upper and lower surfaces of the wing, and the antisymmetrical components being equal in magnitude but opposite in sign in the upper and lower surfaces. Corresponding to the symmetrical stresses and strains will be deflections in the mean chord surface, and corresponding to the antisymmetrical stresses and strains will be deflections normal to the wing. This conveniently divides the work into two separate analyses followed by a coupling procedure, the antisymmetrical components corresponding to bending behavior, and the symmetrical components corresponding to membrane behavior. The bending analysis can be performed without difficulty by standard linear redundant structure techniques. The coupling is necessary because the two types of behavior are interdependent.

### 1. Bending Analysis

The analysis of the structure for bending remains unchanged even though the influence of membrane behavior is being taken into account. Bending deflections can still be determined by the conventional procedure. Assuming that a unit load and strain analysis has been completed for the antisymmetrical components, the bending deflections of the structure are, from Eqs. (3) and (4)

$$\{\delta_m\} = [A_{mn}]_B\{P_n\} + \{\bar{\delta}_m\}$$

The component of deflection due to the antisymmetrical component of thermal strain, $\{\bar{\delta}_m\}$, should be calculated from Eq. (4). For a rectangular arrangement of spars and ribs, the strains $\{\epsilon_j\}_B$ of Eq. (4) are simply

Spars and Ribs

$$\epsilon = (\alpha T)_B \tag{5a}$$

Panels

$$\epsilon = 0 \tag{5b}$$

The subscripts $B$ and $M$, meaning bending and membrane hereafter will be appended wherever desirable to distinguish between matrices corresponding to the two types of behavior. Solving for $\{P_n\}$ and letting $[A_{mn}]_B^{-1} = [K_{mn}]_B$,

$$\{P_n\} = [K_{mn}]_B(\{\delta_m\} - \{\bar{\delta}_m\}) \tag{6}$$

If the membrane effect is included, Eq. (6) still must hold for the part of the total load carried in bending; the latter therefore is given by the right-hand side of Eq. (6). Having this loading, one can solve for the antisymmetrical internal load distribution, using Eq. (2):

$$\{q_i\}_B = [\Gamma_{im}]_B[K_{mn}]_B(\{\delta_m\} - \{\bar{\delta}_m\}) + [\Gamma_{ij}]_B\{\epsilon_j\}_B \tag{7}$$

### 2. Membrane Analysis

Assume temporarily that the structure is capable only of membrane behavior and that it has been placed in a deflected

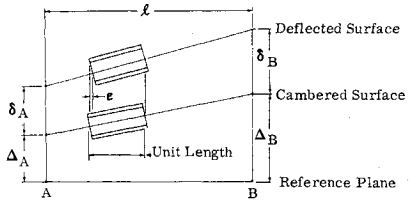


**Fig. 2 Membrane strain in deflected spar**

configuration while remaining statically determinate, so that it is stress free but not continuous. Figure 2 shows schematically a spar segment under these circumstances. Note that the average slope between panel points is taken as the spar slope. Since the distance between panel points $A$ and $B$ has been increased due to deflection from the cambered shape, then, with respect to the deflected surface, the spar segment now has a negative strain. Free thermal expansion due to the symmetric component of $\alpha T$ will add another contribution to the strain. The net strain is denoted by $\epsilon$. The formula for the strain $\epsilon$ can be determined by geometric considerations using a derivation similar to the strain-displacement derivation in shallow shell theory. This results in the following approximate expressions for a spar or rib and for a shear panel in a rectangular arrangement.

Spar or Rib

$$\epsilon = -\frac{1}{2}\left(\frac{\delta_B - \delta_A}{l_{AB}}\right)^2 - \left(\frac{\delta_B - \delta_A}{l_{AB}}\right)\left(\frac{\Delta_B - \Delta_A}{l_{AB}}\right) + (\alpha T)_M \tag{8a}$$

Panel

$$\epsilon = -\frac{1}{2l_{AB}l_{BC}}\left[\frac{1}{2}(\delta_A - \delta_C)^2 - \frac{1}{2}(\delta_B - \delta_D)^2 + (\delta_A - \delta_C)(\Delta_A - \Delta_C) - (\delta_B - \delta_D)(\Delta_B - \Delta_D)\right] \tag{8b}$$

In these formulas $\delta_A$ and $\delta_B$ are the deflections from the cambered shape at the panel points $A$ and $B$ due to both loading and the antisymmetric component of thermal strain, and $\Delta_A$ and $\Delta_B$ are the ordinates of the cambered surface from a chosen reference plane. $(\alpha T)_M$ is the average thermal strain

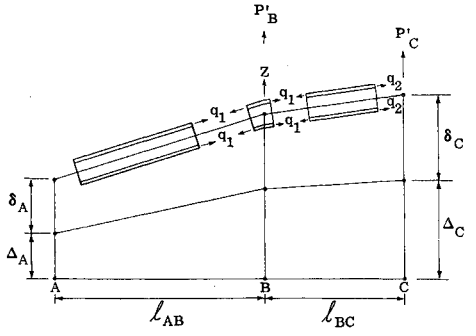


**Fig. 3 Lateral equilibrium of membrane forces in deflected spar**

through the depth of the section, the subscript $M$ denoting membrane component.

With the quantities $\epsilon$ evaluated for all members of the structure, the member-load distribution can be determined easily by making use of the matrix $[\Gamma_{ij}]$, which, as previously stated, gives the member loads throughout the structure due to unit strains existing in the unloaded statically determinate state. The matrix $[\Gamma_{ij}]$ is obtained by performing a plane stress analysis on either surface of the wing using the reference plane geometry. The formula for the member-load distribution including the effects of in-plane applied loads is, from Eq. (2)

$$\{q_i\}_M = [\Gamma_{im}]_M\{P_m\}_M + [\Gamma_{ij}]_M\{\epsilon_j\}_M \tag{9}$$

We now examine the equilibrium of the membrane forces at the panel points in the deflected structure. The calculated membrane load distribution satisfies requirements of equilibrium parallel to the reference plane. However, normal to the reference plane there exist resultant forces which must be taken into account.

Consider, as an illustration, the segment of spar shown schematically in Fig. 3. Again, the average slope between panel points is considered to be the spar slope. To calculate the lateral resultant, denoted by $Z$ in Eq. (10), the vertical components of forces at the panel point are summed. This gives

$$Z = 2q_1\left[\frac{(\delta_A + \Delta_A) - (\delta_B + \Delta_B)}{l_{AB}} - \frac{(\delta_B + \Delta_B) - (\delta_C + \Delta_C)}{l_{BC}}\right] \tag{10}$$

where $2q_1$ is the total load in the upper and lower capstrips, $\delta_A$ and $\Delta_A$, etc. are the components of deflection at the three consecutive panel points and $l_{AB}$ and $l_{BC}$ are the distances between them.

An equivalent equation can be written for the shear panels. Figure 4 shows a pair of warped rectangular shear panels together with their projection on the reference plane. The positions of the four corners are identified by the four panel point deflections. The shear flows $q_1$ have a vertical resultant denoted by $Z'$ in Eq. (11) which is calculated by again summing forces vertically. Thus

$$Z' = 2q_1[2(\delta_A + \Delta_A) - 2(\delta_B + \Delta_B) + 2(\delta_C + \Delta_C) + 2(\delta_D + \Delta_D)] \tag{11}$$

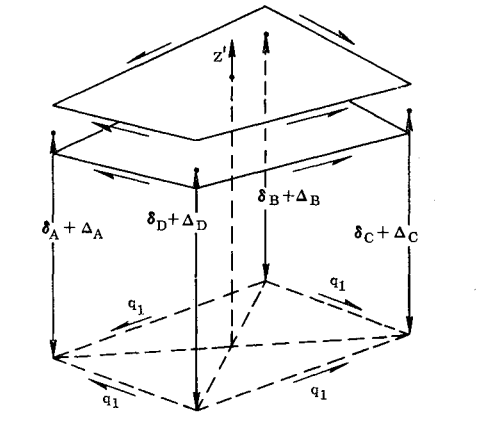


**Fig. 4 Lateral equilibrium of membrane forces in warped shear panels**

The force $Z'$ is assumed to act at the intersection of the diagonals and is replaced, for consistency with the panel point arrangement, by a statically equivalent set of forces at the four corners of the panel. The equilibrants of these resultant forces are the loads carried by the deflected structure acting as a membrane. If there is no applied load but only membrane loads, then the equilibrants become an "apparent" loading induced by deflection and/or camber. The loads sustained can be compiled in matrix form as follows: they are arranged in a column matrix and designated $\{P'_m\}$, each one being the total load at a panel point, i.e., the sum of the equilibrants of $Z$ and $Z'$ from the spars, ribs and shear panels intersecting at the panel point. They are dependent upon the total deflections from the reference plane, which in columnar order, are $\{\delta_n + \Delta_n\}$, and the internal membrane loads that, for convenience of formulation, are written in diagonal matrix form and designated $[q_i]$. A formula relating the loads sustained by membrane behavior to the deflections now can be written as

$$\{P'_m\} = [K_{mn}]_M\{\delta_n + \Delta_n\}$$

where $[K_{mn}]_M$, the stiffness matrix for membrane behavior, is obtained from

$$[K_{mn}]_M = [B_{mi}][q_i][C_{in}] \tag{12}$$

The $[B_{mi}]$ and $[C_{in}]$ matrices consist of geometry dependent constants. Formulas for these constants can be derived from Eqs. (10) and (11). For example, for the spar on the right in Fig. 3, which contributes to the loads sustained at $B$ and $C$, the entries to $[B_{mi}]$ and $[C_{in}]$ are

$$B_{mi} = \begin{matrix} \\ B \\ C \end{matrix}\begin{matrix} \begin{matrix} 1 & 2 \end{matrix} \\ \begin{bmatrix} 2 & 0 \\ 0 & 2 \end{bmatrix} \end{matrix} \quad \text{and} \quad C_{in} = \begin{matrix} \\ 1 \\ 2 \end{matrix}\begin{matrix} \begin{matrix} B & C \end{matrix} \\ \begin{bmatrix} 1/l_{BC} & -1/l_{BC} \\ -1/l_{BC} & 1/l_{BC} \end{bmatrix} \end{matrix}$$

As is customary in the direct assembly of a stiffness matrix, the matrix $[K_{mn}]_M$ is first made up to include rows and columns corresponding to all of the panel points and then reduced to account for support conditions by eliminating appropriate rows and columns.

### 3. Coupling

Now, an equation for the total load sustained by the deflected wing can be written, remembering that $[K_{mn}]_B \cdot \{\delta_n - \bar{\delta}_n\}$ is the part of the applied load resisted by bending. The total load is

$$\{P_n\} = [K_{mn}]_B\{\delta_n - \bar{\delta}_n\} + [K_{mn}]_M\{\delta_n + \Delta_n\} \tag{13}$$

(The matrix $[K_{mn}]_M$ is identical to $-[F_{mn}]$ of a previous paper.[7])

### 4. Tangent Flexibility Matrix

The tangent flexibility matrix corresponding to a particular deflected shape will be defined to be such that an element gives the deflection at one point due to a unit load at another, assuming that the structure deflects linearly from its deflected shape. It is convenient to calculate the tangent flexibility matrix by first obtaining its inverse, the tangent stiffness matrix. If one differentiates Eq. (13) with respect to a particular deflection, $\delta_t$, and bears in mind that $[K_{mn}]_M$ is dependent upon all of the deflections, one obtains the $t$th column

of the required matrix; thus

$$\{\partial P_m/\partial\delta_t\} = \{K_{mt}\}_B + \{K_{mt}\}_M + [\partial K_{mn}/\partial\delta_t]_M\{\delta_n + \Delta_n\}$$

With $\{K_{mt}\}_B$, $\{K_{mt}\}_M$, and $\{\delta_n + \Delta_n\}$ already determined, there remains only the job of calculating $[\partial K_{mn}/\partial\delta_t]_M$. This is obtained from Eq. (12).

$$[\partial K_{mn}/\partial\delta_t]_M = [B_{mi}][\partial q_i/\partial\delta_t][C_{in}] \tag{14}$$

The diagonal matrix in Eq. (14) is obtained by rearranging the result of differentiating Eq. (9). Thus,

$$\{\partial q_i/\partial\delta_t\} = [\Gamma_{ij}]\{\partial\epsilon_j/\partial\delta_t\} \tag{15}$$

The elements of $\{\partial\epsilon_j/\partial\delta_t\}$ are calculated individually for every element in the structure by differentiating Eq. (8).

For compactness, let

$$[\partial K_{mn}/\partial\delta_t]_M\{\delta_n + \Delta_n\} = \{\Delta K_{mt}\}_M \tag{16}$$

If the differentiation is carried out with respect to all of the deflections and the resulting columns of $\{\partial P_m/\partial\delta_t\}$'s are arranged in layers, the entire tangent stiffness matrix, with $t$ now indicating a general deflection is

$$\left\{\frac{\partial P_m}{\partial\delta_t}\right\} = \{K_{mt}\}_B + \{K_{mt}\}_M + \{\Delta K_{mt}\}_M \tag{17}$$

Three-dimensional expansions of Eqs. (14) and (16) corresponding to the complete matrix are

$$\left[\frac{\partial K_{mn}}{\partial\delta_t}\right]_M = [B_{mi}]\left[\frac{\partial q_i}{\partial\delta_t}\right][C_{in}]$$

$$\left[\frac{\partial K_{mn}}{\partial\delta_t}\right]_M\{\delta_n + \Delta_n\} = \{\Delta K_{mt}\}_M \tag{18}$$

Equation (17) now can be written in the more familiar notation as

$$[K_{mn}] = [\partial P_m/\partial\delta_n] = [K_{mn}]_B + [K_{mn}]_M + [\Delta K_{mn}]_M \tag{19}$$

The tangent flexibility matrix is obtained simply from

$$[A_{mn}] = [K_{mn}]^{-1} \tag{20}$$

## IV. Calculation Procedure

### 1. Preliminary Calculations

From the formulas derived in the previous section, an iterative procedure can be established for performing a nonlinear analysis of a cambered wing subjected to applied loading and a thermal environment.

As one preliminary step, a unit load and strain analysis must be performed for both symmetric and antisymmetric components. This phase of the analysis has been discussed in Sec. II and should proceed without difficulty using the formulas and references given. The member flexibilities may have to be different for the two analyses since in one case, the flexibility of a member for bending must be represented and in the other case, the membrane flexibility. The quantities $\{\delta_m\}$ also should be calculated beforehand according to Sec. III, and the flexibility matrix for bending should be inverted for use later as a stiffness matrix.

### 2. General Solution

In Sec. III expressions were derived for the loads sustained by the structure in a prescribed deflected configuration and for the corresponding tangent flexibility matrix and internal load distribution. The problem usually encountered, however, is to calculate these quantities with the loading rather than with the deflections given. Since explicit expressions for solving this problem are not obtainable, a means of arriving at the required result through a series of iterations, beginning with an assumed deflected shape and applying successive corrections, is given. In the absence of a better approximation, one might start the iterations by assuming that the deflections are zero. In some cases it will be necessary to carry out only two cycles of the procedure. The need for a third cycle will be apparent from the result of the second, and so on. The accuracy of the result is readily determined at the completion of each cycle by how nearly the calculated loads sustained by the structure agree with the actual applied loads. If the loads are substantially different, then a set of correcting loads is applied and the structure is assumed to deflect linearly from the present to the improved configuration. This is accomplished as the first step in the succeeding cycle.

The calculation of the loads sustained in a configuration and the flexibility for deflection from that configuration proceeds as discussed in Sec. III. The equation for arriving at an improved configuration, say the $k$th, by linear extrapolation from the $(k-1)$st is

$$\{\delta_m{}^{(k)}\} = \{\delta_m{}^{(k-1)}\} + [A_{mn}{}^{(k-1)}](\{P_n\} - \{P_n{}^{(k-1)}\}) \tag{21}$$

where the superscripts indicate the pertinent cycles, and $\{P_n\}$ without a superscript is the applied loading.

To summarize the procedure, the steps are enumerated below. The preliminary calculations, which only need be performed once, are indicated by an asterisk.

*1) Calculate by unit load and strain analysis for bending, using Eq. (1) and references $[\Gamma_{im}]_B$, $[\Gamma_{ij}]_B$, $[A_{mn}]_B$, and $[A_{mj}]_B$.

*2) Calculate by unit strain analysis, for membrane behavior, using Eq. (1) and references $[\Gamma_{im}]_M$ and $[\Gamma_{ij}]_M$.

*3) Calculate from Eqs. (5) and (4) $\{\epsilon_j\}_B$ and $\{\delta_n\}$.

*4) Invert $[A_{mn}]_B$ to give $[K_{mn}]_B$.

5) Calculate from Eq. (21), for the present ($k$th) cycle interpreting superscript (0) quantities to be zero, $\{\delta_m{}^{(k)}\}$ (thus $\{\delta_m{}^{(1)}\} = 0$).

6) Calculate from Eq. (7) $\{q_i\}_B$.

7) Assemble element-by-element from Eqs. (8) and their derivatives $\{\epsilon_j\}_M$ and $[\partial\epsilon_j/\partial\delta_t]_M$.

8) Calculate from Eqs. (9) and (15) $\{q_i\}_M$ and $[\partial q_i/\partial\delta_t]_M$.

9) Calculate from Eqs (12) and (18) $[K_{mn}]_M$ and $[\Delta K_{mn}]_M$.

10) Calculate from Eqs. (19) and (20) $[A_{mn}{}^{(k)}]$.

11) Calculate from Eq. (13) $\{P_n{}^{(k)}\}$.

The procedure terminates with step 11 in the cycle for which the calculated loads are in agreement with the actual applied loads. The load distributions, deflections, and tangent flexibility matrix determined in that cycle all correspond to the correct deflected configuration.

## V. Example

The calculation procedures previously described now will be illustrated by use of the very much simplified box-beam structure of Fig. 5. Other authors already have treated essentially the same structure for various loadings and various initial deformations.[15–18] The objective here will be to try to emphasize only the ways in which a cambered but untwisted wing may be expected to behave differently from an uncambered one. For this purpose, only a doubly symmetrical applied loading need be considered.

### 1. Idealized Structure and Applied Loads

As can be seen from Fig. 5, the structure is held down on its centerline at the front and rear beams. The box beam is

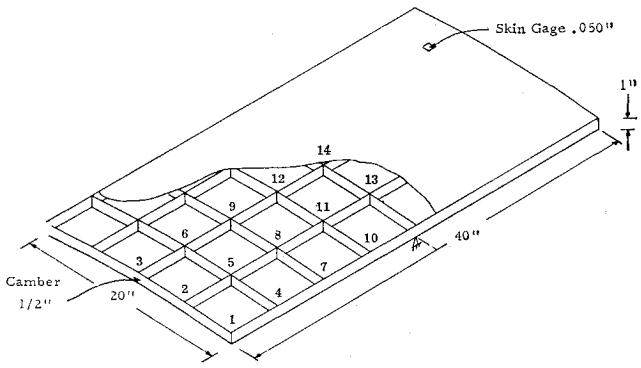


**Fig. 5 Example wing structure**

pictured as having a small amount of camber; it should be thought of as being symmetrical about a mean chord surface. The camber is obtained by displacing the mean chord plane of the uncambered wing into a parabolic surface, with a maximum displacement at the center of $\frac{1}{2}$ in. By so doing, the moment of inertia of the finite-element cross section is increased by approximately 14%, as compared to the idealized, uncambered wing.

In this example, the wing is idealized by lumping the cover material into equivalent stringers over the spars and ribs with the contributions of the spars and ribs themselves assumed to be negligible. The spar and rib webs are assumed to be rigid in shear.

Represented in this way, the structure is redundant 16 times for symmetrical loads, and a total of 14 symmetrically applied loads at the intersections of spars and ribs is considered. These loads are numbered in Fig. 5.

A clamped support condition is simulated by adjusting the applied loads at points 13 and 14 so that the deflections there are zero.

To simplify the comparisons as much as possible, the applied loads $P_m$ in all cases will simulate a uniformly applied lateral pressure $p$. The deflections of the structure will be represented by a single generalized displacement $\delta$ corresponding to $p$, which is defined herein simply by $\delta \times p = [\delta_m]\{P_m\}$. Changes in the quantity $\delta/p$ will be an indication of changes in the structure's flexibility. A more sensitive indicator would be one based upon the tangent flexibility matrix, but $\delta/p$ is more convenient to calculate.

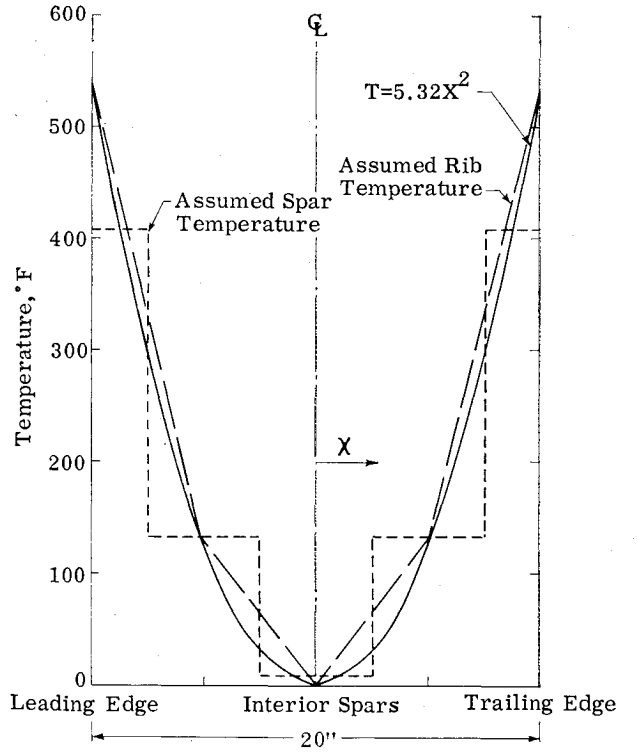


**Fig. 6 Chordwise temperature profile; example wing structure**

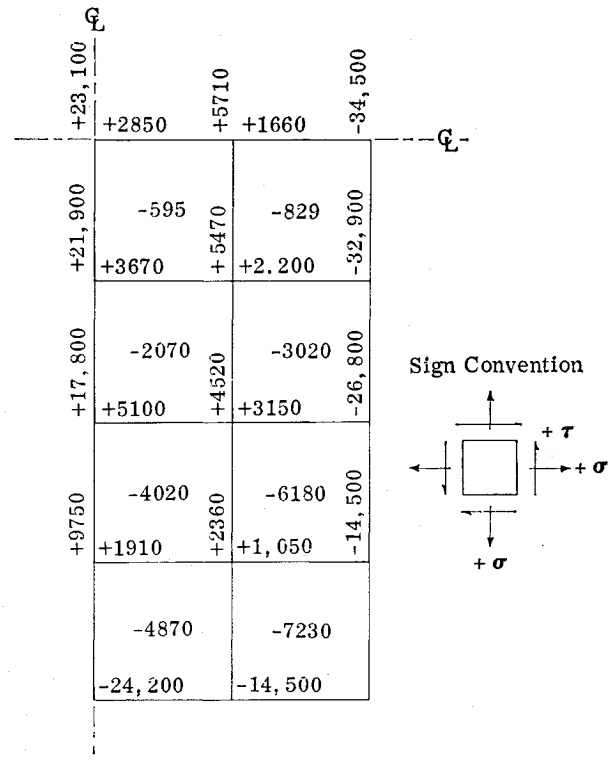


**Fig. 7 Thermal stress distribution; example wing structure**

The dimensions of the structure are shown in Fig. 5. Young's modulus is taken as $10^7$ psi and Poisson's ratio as 0.316.

### 2. Thermal Loading

The temperature distribution to be considered is parabolic in the chordal direction and peaks sharply at the leading and trailing edges, as shown in Fig. 6. It is assumed to be uniform in the spanwise direction. If, in addition, the spar and rib webs are assumed to be able to breathe freely in the spar and rib directions, while remaining rigid in shear, the structure and thermal loading are compatible with that considered in Ref. 15. The temperature level assumed for each of the lumped spars is shown by the stepped curve of Fig. 6. Rib cap temperatures are assumed to vary linearly, as shown.

The modulus of elasticity for an aluminum alloy material would actually deteriorate somewhat at the temperatures shown on Fig. 6. It is nevertheless assumed to remain unchanged from $10^7$ psi in order to emphasize the effects of primary interest. For the same reason, the coefficient of expansion $\alpha$ is also taken to be constant and equal to $15 \times 10^{-6}$ in./in./°F.

Under the preceding conditions, the thermal stresses that result are shown in Fig. 7. The distribution is similar to that of Fig. 11 of Ref. 15; the differences are believed to be attributable mainly to the fact that in Ref. 15 the manner in which the shear panels are attached to the stringers and also the manner in which the temperature variation in the ribs is simulated are somewhat different from herein.

### 3. Clamped Support Condition

The basic case is, of course, the cambered wing with clamped support at room temperature. For $p = 0.1$ psi, the results of the calculation procedure show that the average tip displacement is 0.0068 in., and $\delta/p = 5.51$ in$^5$/lb. The cor-

responding uncambered structure result is $\delta/p = 6.05$, indicating that with camber roughly 91% of the applied load is carried by conventional wing bending, whereas the remainder is carried by membrane action. The membrane action is thus somewhat less than what might be expected based purely upon a comparison of the moments of inertia of the cambered and uncambered structures; the difference is attributed to the proportionately rather large shear flexibilities present in the membrane structure.

When the pressure loading is increased to ±10 psi, the structure shows a slight departure from purely linear behavior. The $\delta/p$ values are given in Table 1; they indicate that the structure stiffens a bit for up loads and becomes a bit more flexible for down loads. An examination of the individual displacements yields the explanation for this. In the case of the upward-acting applied loads, the anticlastic curvature effect increases the camber, and the membrane structure, becoming deeper, thereby is stiffened. For a downward-acting load, the same anticlastic curvature effect tends to decrease the camber and the membrane structure becomes more flexible. The changes are very small because of the root constraint. In the case of the uncambered wing, there is, practically speaking, no change in flexibility as the loading increases from 0.1 to 10 psi.

The maximum stress occurring is in the spanwise direction and at the root, as expected. For the 10 psi loading, up or down, the maximum value is approximately 20,000 psi in the case of the uncambered structure, whereas for the cambered structure it is approximately 31,200.

The cambered wing with clamped support now is subjected to the temperature distribution of Fig. 6. No lateral loading is applied. In the first iteration cycle, the deflections $\delta_m$ are assumed to be zero; the membrane-load distribution that is calculated subsequently in this cycle is thus identical to that for the uncambered structure, as shown in Fig. 7. Subsequent iterations are found to converge practically by the second cycle and completely by the third cycle, with the average deflection at the tip equal to 0.225 in. At the same time the membrane-stress distribution of Fig. 7 has relaxed such that the maximum thermal stress is now 30,800 psi instead of 34,500, and the other stresses have changed in roughly the same proportion.

Applying a 0.1-psi lateral load now to the heated clamped cambered structure, the deflection parameter $\delta/p$ equals 5.54. This is a trifling increase from the corresponding room temperature value of 5.51. When the loading is increased to ±10 psi, $\delta/p$ becomes 5.51 and 5.56, respectively.

**Table 1 Clamped support condition**

| | Lateral Load, psi, (+ up, - down) | δ/p | |
|---|---|---|---|
| | | Room Temp. | Elevated Temp. |
| Uncambered Wing | ± 0.1 | 6.05 | 6.12 |
| | ± 10 | 6.05 | 6.12 |
| Cambered Wing | + 10 | 5.49 | 5.51 |
| | ± 0.1 | 5.51 | 5.54 |
| | - 10 | 5.52 | 5.56 |

**Table 2 Two-point support condition**

| | Lateral Load, psi, (+ up, - down) | δ/p | |
|---|---|---|---|
| | | Room Temp. | Elevated Temp. |
| Uncambered Wing | ± 0.1 | 10.00 | 11.79 |
| | ± 10 | 9.81 | 11.39 |
| Cambered Wing | + 10 | 8.57 | 9.38 |
| | ± 0.1 | 9.29 | 10.37 |
| | - 10 | 9.87 | 11.36 |

In the case of the uncambered clamped root structure, $\delta/p$ increases from 6.05 to 6.12 when thermal effects are included, and is for practical purposes unaffected by load in the range being considered. The increment in flexibility for this latter case would appear to be consistent with the similar case investigated in Ref. 15.

### 4. Two-Point Support Condition

In order to emphasize the importance of the support condition, the investigations previously discussed for the clamped case have been repeated for the two-point support case illustrated in Fig. 5. It is appreciated that this is not an entirely realistic situation, because in an actual design the structure would of necessity be stiffened locally in the region of the tie down attachments. Nevertheless, the true situation should fall somewhere between the two extremes given.

In the case of the uncambered unheated wing, the deflection parameter increases markedly over the clamped root case, now equalling 10.00 for the 0.1-psi loading and 9.81 for 10 psi. (See Table 2.) The slight stiffening with load is due to anticlastic curvature. The bending stress at the root section is now very nonuniform, showing a stress concentration factor of 1.6 directly over the tie down points as compared to the clamped support case.

When the temperature gradient of Fig. 6 is imposed upon the uncambered structure, $\delta/p$ increases by 18% in the case of the 0.1-psi loading, as shown in Table 2. It then exhibits a slightly nonlinear behavior as the loading is raised to 10 psi, stiffening up somewhat, as it should.

When camber is introduced the structure shows the same trends as for the clamped case, except that they now are pronounced much more. Thus for a 10-psi up load at room temperature, the camber at the root increases from an unloaded value of 0.5 to 0.69 in. This results in an appreciable stiffening of the structure, as might be expected. For a 10-psi down load, the camber decreases to 0.28 in., with a corresponding increase in flexibility. These same trends continue when the structure is heated, as indicated by the other $\delta/p$ values of Table 2.

The iteration method again converges very rapidly; in all cases investigated, the results do not change after the third cycle.

The nonlinear behavior of the cambered structure with increasing load (with or without heating) is sufficient in this case to warrant serious consideration. However, other practical design features not included here, such as the local stiffening of the structure in the root region mentioned previously, largely may eliminate these trends.

## References

[1] Denke, P. H., "Digital analysis of non-linear structures by the force method," Structures and Materials Panel, AGARD, NATO, Paris, France (July 6, 1962).

[2] Turner, J. M., Dill, E. M., Martin, H. C., and Melosh, R. J., "Large deflections of structures subjected to heating and external loads," J. Aero/Space Sci. **27**, 97–106 (1960).

[3] Gallagher, R. H., "Matrix structural analysis of heated airframes," Proc. Symp. Aerothermoelasticity, Aeronaut. Systems Div., TR 61-645, p. 879 (October 1961).

[4] Klein, B., "A simple method of matrix structural analysis: Part IV Non-linear problems," J. Aero/Space Sci. **26**, 351–359 (1959).

[5] Lansing, W., Jones, I. W., and Ratner, P., "Non-linear shallow shell analysis by the matrix force method," *Collected Papers on Instability of Shell Structures*, NASA TN D-1510 (1962).

[6] Marguerre, K., "Zur Theorie der gekrummten Platte grosser Formanderung," *Proceedings of the Fifth International Congress of Applied Mechanics* (John Wiley & Sons, Inc., New York, 1939), pp. 93–101.

[7] Lansing, W., Jones, I. W., and Ratner, P., "A matrix force method for analyzing heated wings, including large deflections," *Symposium Proceedings, Structural Dynamics of High Speed Flight, April 1961*, Office of Naval Res. ACR-62, Vol. 1, pp. 533–566 (1962).

[8] Wehle, L. B., Jr. and Lansing, W., "A method for reducing the analysis of complex redundant structures to a routine procedure," J. Aeronaut. Sci. **19**, 677–684 (1952).

[9] Denke, P. H., "A matrix method of structural analysis," *Proceedings of the Second U. S. National Congress of Applied Mechanics* (American Society of Mechanical Engineers, New York, 1945), pp. 445–451.

[10] Argyris, J. H. and Kelsey, S., "The matrix force method of structural analysis and some new applications," Brit. Aeronaut. Res. Council TR Repts. & Memo. no. 3034 (1957).

[11] Grzedzielski, A. L. M., "Organization of a large computation in aircraft stress analysis," Natl. Res. Council Can., Aeronaut. Ret. LR-257 (July 1959).

[12] Grzedzielski, A. L. M., "Theory of multi-spar and multi-rib wing structures," Natl. Res. Council Can., Aeronaut. Rept. LR-297 (January 1961).

[13] Critchelow, W. J. and Haggenmacher, G. W., "The analysis of redundant structures by the use of high-speed digital computers," J. Aeronaut. Sci. **27**, 595–606 (1960).

[14] Bruhn, E. F. and Schmitt, A. F., *Analysis and Design of Aircraft Structures: Analysis of Stress and Strain* (Tri-State Offset Company, Cincinnati, Ohio, 1958), Vol. 1, Chap. A8.

[15] Basin, M. A., MacNeal, R. H., and Shields, J. H., "Direct analog method of analysis of the influence of aerodynamic heating on the static characteristics of thin wings," J. Aerospace Sci. **26**, 145–154 (1959).

[16] Vosteen, L. F. and Fuller, K. E., "Behavior of a cantilever plate under rapid-heating conditions," NACA RM L55E20c (July 1955).

[17] Heldenfels, R. R. and Vosteen, L. F., "Approximate analysis of effects of large deflections and initial twist on torsional stiffness of a cantilever plate subjected to thermal stresses," NACA TN 4067 (August 1957).

[18] Gallagher, R. H., Quinn, J. F., and Padlog, J., "Deformation response determinations for practical heated wing structures," *Symposium Proceedings, Structural Dynamics of High Speed Flight, April 1961*, Office of Naval Res. ACR-62, Vol. 1, pp. 567–608 (1962).


JULY 1963 AIAA JOURNAL VOL. 1, NO. 7

# Optimum Design of Truss-Core Sandwich Cylinders Under Axial Compression

GERALD A. COHEN*

*Aeronutronic Division, Ford Motor Company, Newport Beach, Calif.*

**Sufficient conditions are determined for which equality of the critical stresses is necessary for minimum weight design of compression structures with two instability modes. It is shown that these conditions are satisfied for single and double truss-core sandwich cylinders under axial compression if the sandwich depth is free (i.e., not determined by other considerations, such as wall resistance to meteoroid penetration or heat transfer). Charts are presented which determine minimum weight designs of single and double truss-core sandwich cylinders if the sandwich depth is free. The optimization problem with the sandwich depth given is discussed, but no numerical work has been done to generate design charts for this case.**

## Nomenclature

$A_c$ = cross-sectional area of core per unit of circumferential width
$A_f$ = cross-sectional area of face per unit of circumferential width
$b_c$ = width of core elements
$b_f$ = width of face elements
$E$ = elastic modulus
$h$ = sandwich thickness measured between middle surfaces of face elements
$I_c$ = cross-sectional moment of inertia of core per unit of circumferential width
$I$ = cross-sectional moment of inertia of face per unit of circumferential width
$k_g$ = general buckling coefficient
$k_l$ = local buckling coefficient
$k_{pq}$ = sequence of functions whose minimum (with respect to integral values of $p$ and $q$) is $k_g$
$L$ = length of cylinder
$m$ = index denoting single truss core ($m = 1$) or double truss core ($m = 2$)
$n$ = number of independent geometric variables required to define cross section
$q$ = load per unit width (load intensity)
$R$ = radius of cylinder
$s$ = shear deformation reduction factor
$t$ = thickness of thin-wall cylinder
$\bar{t}$ = cross-sectional area per unit width (effective thickness)
$t_c$ = thickness of core elements
$t_f$ = thickness of face elements
$x_i$ = independent geometric variables that define cross section
$Z,\beta,\zeta,$ $\Lambda,\xi,\psi$ = functions defined in text

Presented at the IAS 31st Annual Meeting, New York, January 21–23, 1963; revision received May 20, 1963. This work was performed under Aeronautical Systems Division Contract AF 33(616)-7775.

* Staff Member, Engineering Analysis Department.